



ELSEVIER

Surface Science 391 (1997) L1205–L1211

surface science

Surface Science Letters

Flux-dependent scaling behavior in Cu(100) submonolayer homoepitaxy

Anna K. Swan *, Zhu-Pei Shi, John F. Wendelken, Zhenyu Zhang

Solid State Division, Oak Ridge National Laboratory, Oak Ridge, TN 37831, USA

Received 19 May 1997; accepted for publication 11 August 1997

Abstract

The average separation of two-dimensional islands in Cu(100) submonolayer homoepitaxy as a function of the deposition flux at 213 K has been studied using spot profile analysis low-energy electron diffraction. As the flux decreases, a large change in the apparent critical island size, from one to a value between seven and 12 atoms, is obtained even though the temperature is held constant. This is shown to be consistent with a recently proposed dimer shearing mechanism which has a significant influence on the stability of islands with eight atoms or less. © 1997 Elsevier Science B.V.

Keywords: Copper; Low energy electron diffraction (LEED); Low index single crystal surface; Scanning tunneling microscopy (STM); Surface diffusion; Surface structure

A great deal of effort has recently been devoted to gaining a fundamental understanding of the early stages of thin-film growth. These early stages are typified by the formation of two-dimensional (2D) islands via the deposition, diffusion, nucleation and aggregation of atoms at submonolayer coverages. As the morphologies and the distributions of the 2D islands may greatly influence the growth mode in the multilayer regime [1], it is highly desirable to learn about the characteristics of the islands, and to identify the crucial atomic processes involved in forming those islands.

The renewed interest in this area stems largely from the fact that quantitative methods for island characterization using real-space microscopy or reciprocal-space diffraction techniques have been

developed. Nevertheless, it is still impossible to observe directly and characterize the nucleation stage of 2D island growth. Instead, one typically resorts to an “archaeological” approach, in which the early-stage nucleation events are inferred by studying the later-stage characteristics of the system. These properties are studied for varying growth conditions, e.g. by measuring the island density as a function of surface temperature or deposition flux. The results can then be compared with the predictions from classical nucleation theory in which the steady-state island density N for high D/F ratios satisfies [2]

$$N \sim \left(\frac{D}{F}\right)^{-p} \exp\left[\frac{E_i}{(i+2)k_B T}\right]. \quad (1)$$

Here D is the adatom diffusion coefficient, F is the deposition flux, $p = i/(i+2)$ (for isotropic diffu-

* Corresponding author. Fax: (+1) 423 576.8135; e-mail: swanak@ornl.gov

sion), T is the surface temperature, and E_i is the cohesive energy of the critical-sized island. The critical island size i is defined as the cluster size that has the lowest nucleation density (highest free energy), and hence it constitutes a “nucleation barrier” for further growth of the islands [3]. D can be expressed in terms of the adatom attempt frequency ν and the activation barrier E_d by $D = \nu \exp(-E_d/k_B T)$.

Eq. (1) is of considerable importance because it holds the promise of experimentally extracting the microscopic parameters ν , E_d and E_i , which otherwise are difficult to obtain. In practice, the application of Eq. (1) to a specific system could be a very demanding exercise, because one must first determine if complicating factors such as anisotropic diffusion [4], motion of small clusters [5,6], and finite-size effects [7] are present. In cases where Eq. (1) is applicable, one central quantity is the critical island size i , which must be determined before it is possible to determine the other intrinsic physical parameters experimentally. The value of i can best be obtained by measuring the island density as a function of deposition flux. The preferred growth condition for determining ν and E_d is clearly when the system is in the irreversible aggregation regime, where $i=1$, typically taking place at low temperatures. The value of E_i is non-zero only when $i>1$. Since E_i contains important new information about adatom–adatom interactions at the surface, efforts have been devoted, both experimentally [8–10] and theoretically [11–15], to studying the transition from $i=1$ to larger values of i .

A simple bond counting argument is often used to calculate the possible critical island sizes. The values of $i>1$ will depend on the substrate geometry [11]. For a triangular geometry, the only cluster sizes to become critical are those whose next size up are particularly stable, i.e. the compact hexagonal clusters [15]. On a square substrate, the compact clusters are formed by $n \times n$ atoms so that clusters of size $i=n^2-1$, for $i>1$ would be expected to be the critical cluster sizes.¹ In particular, it has

been proposed that only the transition from $i=1$ to $i=3$ is possible in submonolayer homoepitaxy on an unreconstructed metal (100) substrate [12]. The prevailing logic to explain the limitation to these two critical sizes is a straightforward bond counting argument. Under conditions in which a single nearest neighbor (nn) adatom–adatom bond is stable, a dimer is stable, islands will form irreversibly, and $i=1$. If one single nn bond becomes unstable, but two nn bonds are still stable, then a tetramer becomes the minimum stable island, and $i=3$. If corner atoms with two nn bonds become unstable, no island of any size would be stable, and a finite critical island size is absent. For Cu(100) and Fe(100) homoepitaxy, where a change in critical island size has been observed, the transition has been suggested to be from the regime $i=1$ to $i=3$ [8,9]. In these experiments, the transition was induced by increasing the growth temperature, which changes the ratio between every pair of intrinsic rate processes. This complication, plus the coexistence of many active atomistic processes at higher temperatures, leaves much room for debate whenever an application to the case of $i>1$ is made [6,12–14].

One such controversy exists in the case of Cu on Cu(100). The $i=3$ regime for Cu/Cu(100) was identified using spot profile analysis low-energy electron diffraction (SPA-LEED) [16] by Zuo et al. [8], who observed a change in the power-law dependence of $N \sim F^p$ from $p \approx \frac{1}{3}$ to $p \approx \frac{3}{5}$, induced by an increase in growth temperature. Aided by embedded-atom calculations of the cohesive energy of islands of varying size [8,17], the change in p was interpreted as due to a direct increase in the critical island size from $i=1$ at low temperature to $i=3$ at high temperature. This identification seemed to be quite sensible and is consistent with the bond counting argument discussed above. This bond-counting argument has in fact been implied in both cases where $i=3$ was suggested [8,9]. However, the identification of $i=3$ for Cu/Cu(100) has been questioned by Bartelt et al. [12] in a recent model study of metal (100) homoepitaxy. Based on an estimate for the average Cu–Cu bond energy, Bartelt et al. concluded that $i=3$ would occur in a temperature range too small to permit likely observation of this regime.

¹ The bond counting argument implies that $i=s-1$, where s is a cluster size that is particularly stable. While this often is the case, it does not have to be (see Ref. [15]).

In this study, we use SPA-LEED augmented by scanning tunneling microscopy (STM) to characterize the islands formed in Cu(100) homoepitaxy. By reducing the deposition flux at constant temperature, we observe an unexpectedly large increase in apparent critical island size, from one to a value between seven and 12 atoms, without any well-defined intermediate value. The inability to explain this principal experimental finding within the established models stimulated the discovery of dimer shearing as a crucially important atomic process in controlling dynamical island growth [18].

Some aspects of the experimental details have been published previously [8,10]. Briefly, we use a SPA-LEED instrument to measure quantitatively the average island separation at different growth conditions, and an Omicron STM to provide verification of the SPA-LEED results at selective growth conditions. The average terrace width of the Cu(100) surface was estimated to be ~ 700 Å from diffraction measurements. A detailed STM examination of this same surface, based on a random sampling of over 500 terraces scattered across a 4 mm range, indicates an average terrace width of 850 Å. Terraces as wide as 6000 Å were observed. More importantly, the average island site is on a 1880 Å wide terrace, a consequence of the fact that wide terraces hold more islands than narrow ones. Evaporation of Cu onto the sample was performed with an Omicron e-beam evaporator which contains an integrated flux monitor allowing for precise control of a stable flux during deposition. The quantitative flux was determined after each exposure by determination of the coverage from diffraction intensities. The vacuum chamber pressure during evaporation was typically 7×10^{-11} Torr.

The advantage of using the SPA-LEED for quantitative studies of dynamical growth lies in the large area sampled in every diffraction profile measurement (as defined by the spot size of 1 mm^2), high speed data acquisition, and ease in sample temperature control. In the out-of-phase condition (defined for scattering from terraces separated by one atomic height), a first-order diffraction ring becomes detectable around the specular peak, as reported by Henzler and coworkers

[16]. The circular shape of the ring shows that the island distribution is isotropic on the surface, as confirmed by STM images which in addition show predominantly square-shaped compact islands, due to fast edge diffusion (faster than terrace diffusion) [10,19]. The diameter S of the Henzler ring is inversely proportional to the average island separation L , given by $L = 4\pi/S$ [8,10,20,21]. An earlier SPA-LEED study [10], correlating the island sizes and island separations with the coverage, has shown that the assignment of L as the average island separation is correct within a constant of order 1. Here, we have also checked values of L from SPA-LEED against the island density estimated from typical STM micrographs obtained at the same growth conditions, and found that the relation $N_{\text{STM}} \sim L_{\text{LEED}}^{-2}$ holds within 10%.

The main experimental results are summarized in Figs. 1 and 2. In Fig. 1, a log-log plot of the average island separation as a function of the inverse deposition flux at a constant growth temperature of 213 K and a constant coverage of 0.3 ML is shown. With $\nu \sim 10^{12} \text{ s}^{-1}$ and $E_d = 0.36 \text{ eV}$ [10], the flux range spans values of D/F from 2×10^5 to 8×10^7 . Two line segments must be used to fit the data. For fluxes faster than $1/85 \text{ ML min}^{-1}$ (the high-flux regime), the expo-

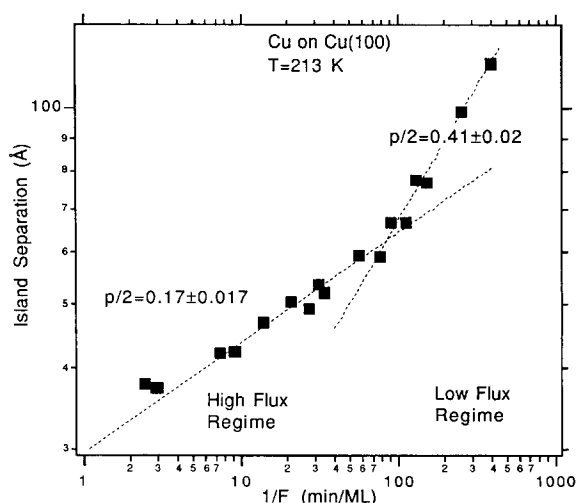


Fig. 1. Log-log plot of the average island separation L vs. the inverse flux F at a constant temperature of 213 K and a constant coverage of 0.3 ML.

ment obtained is $p = \frac{1}{3} \pm 0.03$, given by twice the slope. The value of $\frac{1}{3}$ for the exponent in the high-flux regime corresponds to a critical nucleation size of $i=1$, the expected result at this growth temperature [8]. For fluxes slower than $1/85 \text{ ML min}^{-1}$ (the slow-flux regime), the exponent obtained is $p = 0.82 \pm 0.04$ which corresponds to a critical island size in the range of $i=7-12$ atoms according to Eq. (1).

The island separation as a function of the coverage has also been studied for several deposition rates in both the high- and low-flux regimes (Fig. 2). The curves in the two regimes show qualitatively different behaviors. In the low-flux regime, the data exhibit a minimum in the island separation, i.e. a saturation in the island density, at about 0.3 ML. However, in the high-flux regime, the saturation maximum occurs below 0.2 ML, the lower limit of the range of observation. The results in the high-flux regime are consistent with recent computer simulations, which, by assuming $i=1$, show saturation coverages of less than 0.15 ML, with lower rates resulting in lower saturation cov-

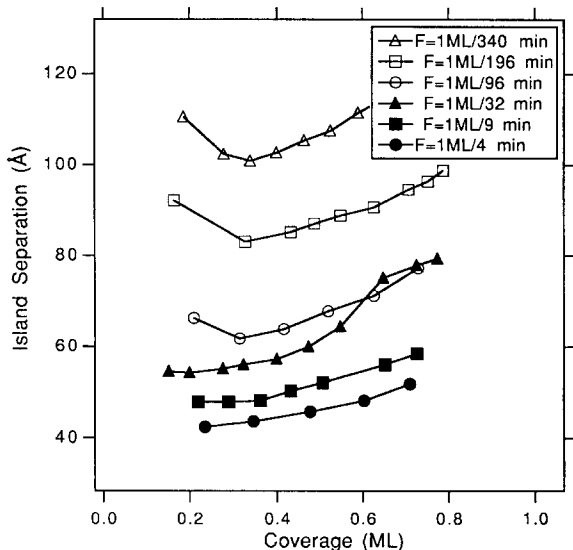


Fig. 2. The dependence of the average island separation on the coverage for varying flux. A minimum in the island separation corresponds to a maximum in the island density (the saturation density). In the low-flux regime (open symbols), the minimum island separation is reached at 0.3 ML. For high fluxes (filled symbols), the saturation density is below the detection limit of ~ 0.2 ML.

erages [22]. However, the results in the low-flux regime are at odds with the $i=1$ prediction: a much higher saturation coverage is observed when the flux is sufficiently low. This is a further indication that a change in nucleation mechanism has occurred. Qualitatively, the shift towards the unusually large saturation coverage in the low-flux regime could be associated with a sizable increase in the critical cluster size. These results came as a surprise. First, the changes observed in critical island size are typically associated with a temperature change; secondly, the magnitude of the slope is too large to fit in the conventional bond counting picture of critical island size. Hence other explanations must be considered.

Experimental artifacts must first be ruled out before attempting to associate the large change in slope with a possibly new dynamical process(es). Step edges act as sinks for adatoms, leading to a depletion zone near the steps. STM micrographs show that the depletion zone is approximately equal to the average island spacing near an up-step and almost non-existent near a down-step (see discussion in Ref. [3]). The average island spacing is, at most, about 120 \AA at the slowest flux in this experiment. Since the typical islands contributing to the observed diffraction features are found on a terrace 1850 \AA wide, the effect of the steps should be minimal. Another possibility is that impurities adsorbed during the long evaporation time on a cold substrate might affect the growth process. Two liquid-nitrogen dewars in the system are colder and provide effective pumping of condensable gases. With the system pressure of 7×10^{-11} Torr during evaporation, the equivalent of ~ 0.5 ML will impact the surface during the 2 h exposure using the slowest evaporation rate. However, the overwhelming fraction of ambient gas is H_2 , which will not adsorb. Most impurities, with the exception of atomic hydrogen [23], can in fact be expected to create nucleation sites, which would result in just the opposite effect to what is observed here. Furthermore, any such small step-edge or contamination effect is bound to produce a gradual change in slope rather than the distinct and large change observed at the island spacing of $\sim 65 \text{ \AA}$. The onset of coarsening should also be considered. To examine coarsening effects, we observed the island spacing at 0.3 ML for over

400 min. During this time, a barely noticeable change in the island separation could be detected, ruling out significant coarsening at 213 K after the steady state island growth regime is obtained. This check does not exclude the possibility of small clusters disappearing via diffusion and coalescence during the nucleation stage. In that case, the exponent p in Eq. (1) will also change. The impact of cluster motion on the scaling behavior has been addressed in a study [5] and it was found that the exponent p asymptotically approaches an upper limit of $p=0.5$ for diffusing clusters of larger and larger sizes. This value is much lower than what we observe ($p=0.82$), which suggests that diffusion does not have a significant impact in determining the island distribution in the present case.

The experimental results discussed above indicate that large clusters, up to size $i=7-12$ atoms, are no longer stable as the flux becomes sufficiently low. This poses questions about how a decreasing flux affects the cluster stability, how such a large cluster can dissociate, and why no $i=3$ regime is observed. These issues are addressed below.

The notion of critical island size is a thermodynamic concept, and a change of i is typically associated with an increase of T , causing thermally activated bond breaking; but this picture is incomplete. Whether a cluster of i atoms is more likely to grow than to fall apart is determined by the number of possible configurations and the cohesive energies of all the accessible states. A state is treated as accessible unless it is excluded by the specifications of the system and the time scale of the measurement [24]. A decrease in flux increases the time scale, thereby making a state kinetically accessible, so that an increase in the value of i may take place.²

The change from $i=1$ to $i=7-12$ in the low flux regime requires a low energy pathway to enable dissociation of clusters of size i and smaller. Removing an atom from a compact cluster involves breaking two nn bonds, which is costly and not likely to happen in the relevant time scales in this experiment. Searching for a kinetic dissoci-

ation pathway leads to the consideration of a process where two atoms are moving together along an edge, dimer shearing [18], as illustrated in Fig. 3b. If dimer shearing is an accessible low energy pathway to dissociation, all clusters smaller than 3×3 atoms can dissociate via dimer shearing and/or single bond scission. In this scenario, a 3×3 cluster will be particularly stable, suggesting that $i=8$.³ A critical island size of $i=8$ yields $p=0.8$, close to the observed value of 0.82 ± 0.04 . Using embedded atom (EAM) calculations we found that the barrier for dimer shearing in a tetramer on Cu(100) is 0.69 eV (Fig. 3b) compared with 0.82 eV for a single atom motion involving double bond scission (Fig. 3a). Similar results are obtained for dimer and single atom motion in clusters of size six and eight. In the compact 3×3 cluster, dimer shearing is not active and a single atom faces a high initial barrier of 0.86 eV for dissociation.

It is desirable to obtain a quantitative estimate of the time scale for the onset of dimer shearing using the results of the EAM calculations. Specifically, if we use $E_{DS}=0.69$ eV, and assume an attempt frequency of 10^{12} s^{-1} , then at 213 K

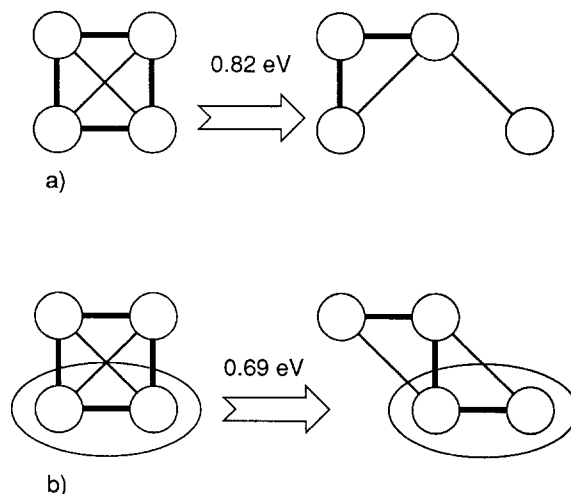


Fig. 3. Activation barriers for the rate-limiting step towards diffusion or dissociation of a Cu tetramer island on Cu(100) via (a) sequential motion of individual atoms, and (b) dimer shearing.

² In Ref. [12], a variable Y is used to follow the change of $i=1$ to $i=3$ for several systems on a square lattice. At constant temperature, Y is proportional to $1/F$.

³ See footnote 1.

we obtain a time scale of 6 h, which is too large compared with our flux-determined time scale. On the other hand, we notice that the EAM calculations, while in many cases are capable of giving qualitatively reasonable results, may have systematically overestimated the activation barriers. This can be seen by comparing the measured activation barrier for single adatom diffusion, 0.36 eV [10], with the calculated value, 0.50 eV. If we use the difference of 0.14 eV as a crude estimate of the systematic error, then the activation barrier for dimer shearing becomes 0.55 eV, and the corresponding time scale for dimer shearing can be estimated to be ~ 0.2 min. This has to be compared with the time between arrival of ad-atoms to the cluster, which is determined by the flux and average terrace area per island. At the onset of the change in slope, $F=1$ ML/86 min and the average island separation is ~ 62 Å, corresponding to a time separation between arriving atoms in one island area of ~ 1.5 min. Here, both the magnitude of the attempt frequency and dimer shearing barrier are reasonable, but crude, estimates; nonetheless, it illustrates that onset of dimer shear with lowered flux is likely to take place. However, it is important to note that the existence of a low energy pathway towards dissociation is a necessary but not a sufficient condition for significant cluster dissociation. In order for dimer shearing to have any impact, a sizable fraction of the clusters (of size less than nine) has to be in a non-compact configuration (configuration where at least one atom is connected to the cluster by only one nn bond). The non-compact configuration is important here because it provides the starting point for dissociation via single nn bond scission.

For a given island size, the difference in binding energy between non-compact and compact configurations, together with the difference in configuration space, determines the relative population of compact and non-compact configurations. Although the binding energy is higher for the compact clusters, and hence favors the compact shape, the configuration space opened up by access to non-compact shapes may significantly enhance the probability of finding a cluster in a non-compact configuration. For the purpose of considering dissociation, not only the sheared configuration of a compact cluster has to be considered,

but also all other non-compact configurations that can easily be reached from the sheared configuration. The contributions to the configuration space for non-compact cluster shapes can be divided into: (a) contributions from all the possible locations on the lattice, n^2 where $n \approx L/a$ (sheared clusters are mobile); (b) a number of different configurations (sheared configurations and others reached from the sheared configurations); (c) a number of atoms attached to the cluster by a single nn bond. In comparison, a stationary compact cluster has only one configuration. Hence, the larger phase space of a non-compact cluster increases the probability for finding a sizable fraction of clusters in a non-compact configuration.

Assuming now that a sizable fraction of compact clusters exists in a non-compact configuration, such a cluster can dissociate by single-bond scission. The dissociation of a non-compact cluster is related to that of a dimer or trimer, since the effective energy barrier for dissociation of a non-compact cluster is similar to that of a dimer or trimer. The effective dissociation energy E_{diss} can be written [12] $E_{\text{diss}} = E_{\text{d}} + \partial E_{\text{b}}$. For small non-compact clusters on Cu(100), the difference in binding energy between the non-compact cluster and the dissociated non-compact cluster, ∂E_{b} varies between 0.25 eV (dimer) and 0.38 eV (seven atoms) and E_{d} was calculated to be 0.4 eV, so that $0.65 \text{ eV} \leq E_{\text{diss}} \leq 0.78 \text{ eV}$ for small non-compact clusters [12]. Comparing the calculated value of the dimer shearing energy barrier E_{DS} with E_{diss} , we find that it is comparable with, or lower than, the effective dissociation energy for non-compact clusters, $E_{\text{DS}} = 0.69$ eV (or lower, see above) and $0.65 \text{ eV} \leq E_{\text{diss}} \leq 0.78 \text{ eV}$. Hence, dimer-shearing appears to set in at, or before, dissociation via single bond scission. With decreasing flux, onset of dimer-shearing may take place before onset of single nn bond dissociation. This order of events would explain the lack of the $i=3$ regime, notably absent in this experiment: once dimers and trimers can dissociate, so can the sheared larger clusters. However, to determine conclusively whether the onset of dimer shearing is relevant to the observed change of slope, a properly formulated nucleation theory calculation would be necessary, but such a

calculation is beyond the scope of the present study.

It is difficult to reconcile the results obtained for this system, i.e. the absence of the $i=3$ regime when decreasing the deposition flux with the earlier observation of the $i=1$ to $i=3$ transition induced by an increase in growth temperature in the same system [8]. Here we only wish to point out that, generally, it is more difficult to interpret results from temperature-dependent studies. In such studies, as the temperature increases, some unknown processes can be turned on, and all the relative time scales will change. Both effects will complicate the interpretations.

To summarize, we have reported the first observation of a flux-induced change in critical island size, at constant temperature, in Cu(100) submonolayer homoepitaxy. The magnitude of this change, from $i=1$ to $i=7-12$, could not be understood in terms of sequential motion of individual atoms and prompted the consideration of dimer shearing as an important dynamical process in metal (100) homoepitaxy. EAM calculations show that dimer shearing provides the necessary low energy pathway to a sheared configuration. We argue that the large increase in configuration space opened up by dimer shearing ensures a significant fraction of compact clusters will exist in a non-compact configuration so that dissociation via single bond scission can take place. Furthermore, the effective dissociation energy for a non-compact cluster of size less than nine atoms is similar to the effective dissociation barrier of a dimer. Hence, the experimental results which indicate a missing $i=3$ regime, and the calculated values of the effective dissociation energy and the dimer shearing barrier, suggest that, with decreasing flux, the onset of dimer-shearing takes place before, or at, the onset of single nn bond dissociation.

Acknowledgements

We would like to thank M.C. Bartelt, M. Breeman, J.W. Evans, S.D. Liu, J. Tersoff, J.A. Venables and A. Zangwill for helpful discussions. This research was sponsored by the Division of Materials Sciences, US Department of Energy

under contract DE-AC05-96OR22464 with Lockheed Martin Energy Research Corp.

References

- [1] R. Kunkel, B. Poelsema, L.K. Verheij, G. Comsa, Phys. Rev. Lett. 65 (1990) 733. G. Rosenfeld et al., Phys. Rev. Lett. 71 (1993) 895. Z.Y. Zhang, M.G. Lagally, Phys. Rev. Lett. 72 (1994) 693.
- [2] J.A. Venables, Philos. Mag. 27 (1973) 697. J.A. Venables, G.D.T. Spiller, M. Hanbücken, Rep. Prog. Phys. 47 (1984) 399.
- [3] J.A. Venables, Surf. Sci. 299–300 (1994) 798. J.A. Venables, Growth and properties of epitaxial thin films, in: D.A. King, D.P. Woodruff (Eds.), Chemical Physics of Solid Surfaces, vol. 8, Chapter 2, Elsevier, Amsterdam, in press.
- [4] M.C. Bartelt, J.W. Evans, Europhys. Lett. 21 (1993) 99. S. Günther, E. Kopatzki, M.C. Bartelt, J.W. Evans, R.J. Behm, Phys. Rev. Lett. 73 (1994) 553. T.R. Linderoth, J.J. Mortensen, K.W. Jacobsen, E. Laegsgaard, I. Stensgaard, F. Besenbacher, Phys. Rev. Lett. 77 (1996) 87.
- [5] J. Villain, A. Pimpinelli, L.H. Tang, D. Wolf, J. Phys. I Fr. 2 (1992) 2107. J. Villain, A. Pimpinelli, D. Wolf, Commun. Condens. Matter Phys. 16 (1992) 1.
- [6] A.D. Gates, J.L. Robins, Surf. Sci. 194 (1988) 13. S. Liu, L. Bonig, H. Metiu, Phys. Rev. B 52 (1995) 2907. L. Bonig, S. Liu, H. Metiu, Surf. Sci. 365 (1996) 87.
- [7] K. Roos, M.C. Tringides, Surf. Sci. 355 (1996) L259.
- [8] J.-K. Zuo, J.F. Wendelken, H. Dürr, C.-L. Liu, Phys. Rev. Lett. 72 (1994) 3064.
- [9] J. Stroschio, D. Pierce, Phys. Rev. B 49 (1994) 8522.
- [10] H. Dürr, J.F. Wendelken, J.-K. Zuo, Surf. Sci. 328 (1995) L527.
- [11] J.A. Venables, Vacuum 33 (1983) 701. J.G. Amar, F. Family, Phys. Rev. Lett. 74 (1995) 2066.
- [12] M.C. Bartelt, L.S. Perkins, J.W. Evans, Surf. Sci. 344 (1995) L1193.
- [13] C. Ratsch, P. Smilauer, A. Zangwill, D.D. Vvedensky, Surf. Sci. 329 (1995) L599.
- [14] P.J. Feibelman, Phys. Rev. B 52 (1995) 12444.
- [15] J.A. Venables, Phys. Rev. B 36 (1987) 4153.
- [16] P. Hahn, J. Clabes, M. Henzler, J. Appl. Phys. 51 (1980) 2079.
- [17] C.L. Liu, Surf. Sci. 316 (1994) 294.
- [18] Z.-P. Shi, Z.Y. Zhang, A.K. Swan, J.F. Wendelken, Phys. Rev. Lett. 76 (1996) 4927.
- [19] Z. Zhang, X. Chen, M.G. Lagally, Phys. Rev. Lett. 73 (1994) 1829.
- [20] H.J. Ernst, F. Fabre, J. Lapujoulade, Phys. Rev. B 46 (1992) 1929.
- [21] M.C. Bartelt, J.W. Evans, Surf. Sci. 298 (1993) 421.
- [22] G.T. Barkema, O. Biham, M. Breeman, D.O. Boerma, G. Vidali, Surf. Sci. 306 (1994) L569.
- [23] K. Haug, Z.Y. Zhang, J. David, C.F. Walters, D.M. Zehner, W.E. Plummer, Phys. Rev. B, in press.
- [24] C. Kittel, H. Kroemer, Thermal Physics, Freeman, 1980, p. 29.